JMEPEG (2012) 21:1193–1198
DOI: 10.1007/s11665-011-0012-3

1059-9495/$19.00

Experimental Study of Thermal and Flame Front Characteristics in Combustion Synthesis of Porous Ni-Ti Intermetallic Material

Zhiliang Li and Olusegun J. Ilegbusi

(Submitted January 27, 2011; in revised form June 15, 2011)

This article describes experimental investigation of thermal and combustion phenomena during the self-propagating combustion synthesis of Ni-Ti intermetallic materials for structural application. Ni-Ti mixture is prepared from elemental powders of Ni and Ti. The mixture is pressed into solid cylindrical samples of 1.1-cm diameter and 2-3-cm length, with initial porosity ranging from 30 to 42%. The samples are pre-heated to various initial temperatures and ignited from the top surface such that the flame propagates axially downward. The flame speed images are recorded with a motion camera, and the temperature profile is recorded. The flame front propagation velocity is deduced as a function of the preheat temperature and initial porosity as well as the effective thermal conductivity of the reactants.

Keywords bio-implant material, combustion synthesis, intermetallic

1. Introduction

The production of certain ceramics, intermetallics, and composite materials by self-propagating high-temperature synthesis (SHS) has become increasingly popular because of its many advantages over conventional processing techniques. These benefits include low cost/energy requirements, high homogeneity of the product, reduced microstructural segregation, low contamination, and the relative simplicity of the process (Ref 1-5). The growing popularity of SHS has led to a number of experimental, theoretical, and numerical studies aimed at improving fundamental understanding of the process (Ref 1-7). However, existing theoretical and numerical studies have typically relied on oversimplifications such as the assumption of constant thermal conductivity throughout the specimen. Further study is therefore necessary to elucidate the effects of process parameters and variable thermophysical properties on the synthesis. This is the primary objective of the present article.

By definition, SHS involves initiating an exothermic, condensed-phase chemical reaction between two or more species to obtain the desired product. Although under the appropriate conditions the exothermic nature of the reaction allows the process to become steadily self-sustaining, SHS is very sensitive to the process parameters and material properties, and other reaction patterns are possible including oscillatory propagation, fingering, and reaction extinction (Ref 8-11).

Zhiliang Li and **Olusegun J. Ilegbusi,** Department of Mechanical, Materials and Aerospace Engineering, University of Central Florida, Orlando, FL 32816-2450. Contact e-mails: zli@knights.ucf.edu and ilegbusi@mail.ucf.edu.

In order to fully realize the potential of SHS, it is imperative that the individual and cumulative effects of the various material and process parameters on the characteristics of both the reaction and the final product be fully understood. Process parameters such as preheat temperature, porosity, and the amount of reactant dilution, have all been shown experimentally to play a significant role on the combustion synthesis (Ref 3, 4, 9, 12-17). The material properties of the various phases also influence the reaction (Ref 7, 9, 17, 18). Experimental data and numerical analysis both suggest that the effective thermal conductivity, k_{eff}, is one of the most important parameters impacting reaction behavior during combustion synthesis (Ref 3, 8, 14, 19, 20). There have therefore been numerous attempts to model SHS through numerical and physical experiments and to apply the existing knowledge for optimization of industrial SHS processes.

In the present study, an experimental apparatus is set up and used to investigate Ni-Ti intermetallic processing using combustion synthesis. It focuses at this stage on the effect of processing conditions on the flame front propagation speed as well as the effect of initial porosity on the effective thermal conductivity. Specifically, compressed Ni-Ti powder cylindrical samples are ignited and used for investigating the flame speed and effective thermal conductivity over a range of initial sample porosities. The flame front propagation speed largely determines the final product porosity and structural properties.

2. Problem Considered

Figure 1 illustrates the combustion synthesis process and the associated differences in effective thermal conductivities for the reactant, combustion, and product phases. Although in practice these differences in thermal conductivity may be either material or process dependent, the exact source is of less concern than the overall effect on the propagation of the reaction front (Ref 21). The source will thus not be specifically addressed in this article.

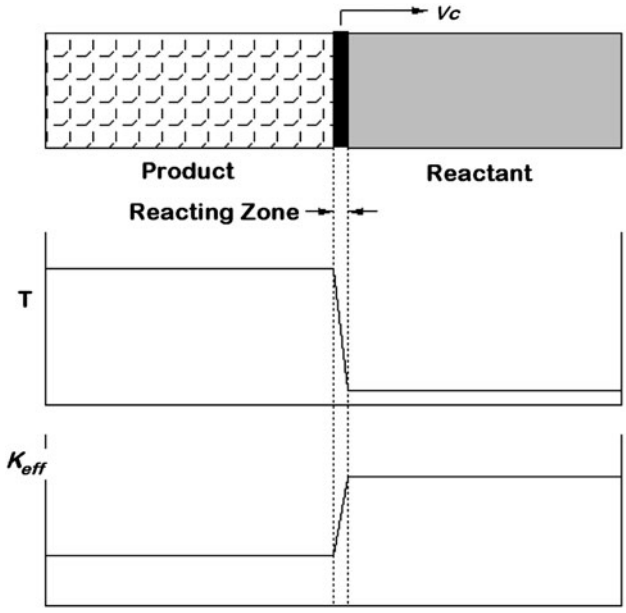

Fig. 1 Schematic of the combustion synthesis process, the corresponding temperature profile, and the effective thermal conductivities for the reactant, combustion, and product regions

3. Experimental Apparatus and Procedure

Figure 2 shows the experimental apparatus used for the study. It consists of a stainless steel iso-velocity Argon flow controller, an insulator, a heating wire, an ignition wire, a motion camera, and an infrared sensor. Cylindrical samples of Ni-Ti intermetallic were prepared from elemental powders of Ni (99.9% purity, 100 mesh, and particle size $\leq$ 0.149 mm) and Ti (99.5% purity, 100 mesh, and particle size $\leq$ 0.149 mm), homogeneously dry-mixed in the stoichiometric ratio of 1:1 in Argon flow purging environment. The powders were cold pressed into cylindrical samples (1.11-cm diameter) with the CARVER manual hydraulic press. The press exerts force on the top surface of the sample, ranging from 3000 to 7000 lb. The corresponding porosities of the samples ranged from 42 to 30%. All the tests were carried out in the Argon flow controller in an open-air environment and monitored with a Redlake Motion camera and an infrared temperature sensor. Each Ni-Ti sample was set on top of an insulator situated within a solenoid Nichrome heating coil. The heating was controlled by a DC power supply (HY3030E) with the capability to uniformly preheat the sample to any prescribed temperature of up to 700 °C within 10 min.

A zigzag tungsten ignition wire (0.5-mm diameter) was set up approximately 2 mm above the top surface of the sample. The ignition current was controlled by another DC power supply (HY3050E). The ignition energy was delivered by radiation heat transfer through the 2-mm gap between the ignition wire and sample surface. The preheating and combustion temperature were acquired using infrared sensor (MICRO EPSILON, thermometer CTM-2). The temperature data were gathered by the data-acquisition system at an interval of 10 ms via a USB interface. In addition, in order to verify the accuracy of the infrared sensor and adjust the material emissivity coefficient, a thermocouple (OMEGA, K type, bead size of 0.12 mm, and response time of about 10 ms) was used to probe

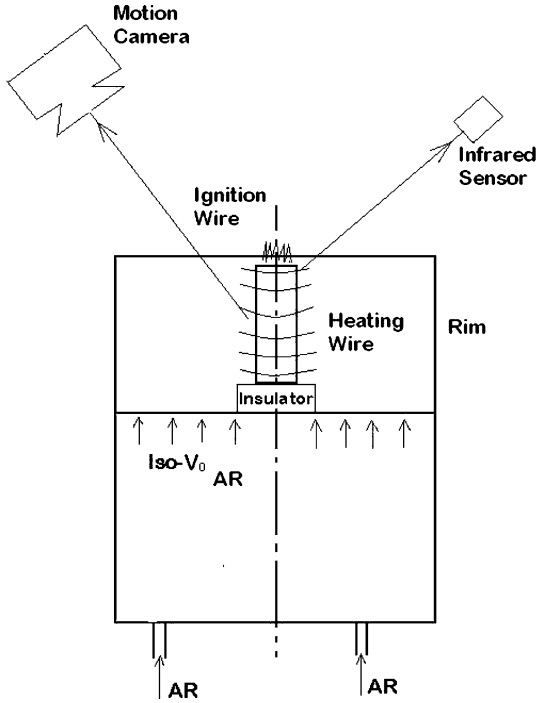

Fig. 2 Schematic of experimental apparatus

the sample surface several times before the ignition. The combustion front propagation speed was then determined from the images of the reaction front position, which was recorded by the motion camera system at a frequency of 50 f/s.

4. CFD-AIDED Design of Argon Purge Flow Control

The top surface of the experimental apparatus was designed to be exposed to air ambience for convenient observation of temperature and flame speed data, as well as to ease the preheating and ignition power cable connection. Thus, argon flow was needed to purge oxygen from the Ni-Ti sample surface. A certain average flow velocity (V_0) would be required to ensure that the oxygen fraction on the sample surface was negligible while also minimizing the argon consumption and heat loss.

A Computational Fluid Dynamics (CFD) model was therefore utilized to predict the argon flow velocity V_0 for design of the experiment. For a typical experimental process, the preheating time usually endures for 10 min, the ignition process lasts for 10-60 s, and the flame front propagates from the top to the bottom in about 3 s. Thus, our main concern of inadvertent oxidization was in the preheating phase. For simplification, two representative steady-state simulations were considered in the preheating phase. Table 1 summarizes the boundary conditions used in the two sets of cases.

The preliminary calculations done using CFD are presented in Fig. 3 and 4 for low and high preheating temperatures, respectively. Specifically, the figures present the predicted distribution of oxygen mole fraction as a function of axial and radial positions, x and r respectively, around the sample. Each figure shows results for two average argon velocities, V_0 = 2 cm/s and V_0 = 3 cm/s. The predictions show that for both the low and high preheating temperature simulations, the

Table 1 Boundary conditions used in simulation cases

	Low preheating temperature, °C	High preheating temperature, °C
Heating wire	630	930
Ni-Ti cylinder surface	330	550
Insulator surface	130	230

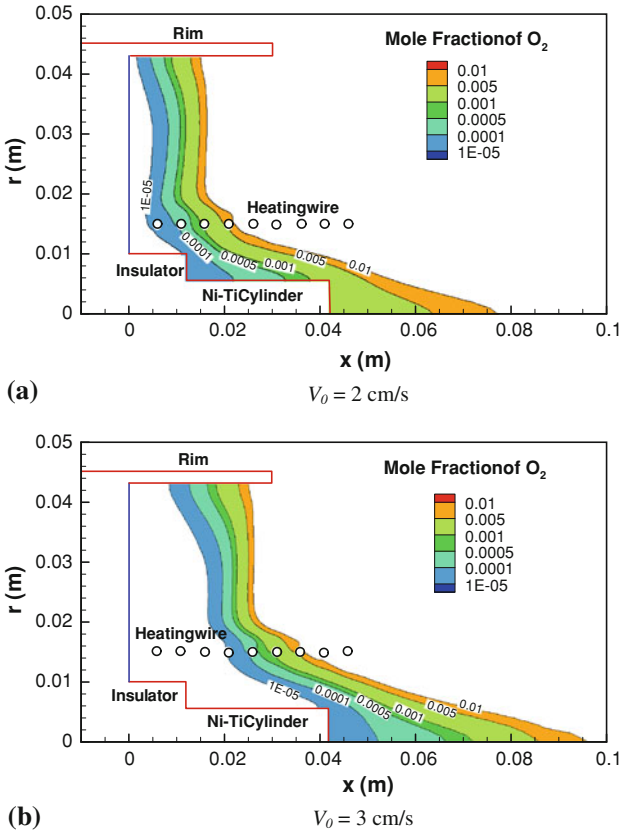

Fig. 3 Contours of mole fraction of oxygen for V_0 = 2 and 3 cm/s in low preheating state

maximum mole fractions of oxygen on the Ni-Ti sample surface would fall below 0.01% for the average argon flow velocity V_0 = 3 cm/s. This flow velocity significantly improves the purging effect compared to the situation with V_0 = 2 cm/s. A velocity of 3 cm/s was therefore considered sufficient for argon purging to ensure negligible oxygen environment, and was so selected for the experiment.

5. Result and Discussion

The processing parameters, including the sample porosity, particle size, and preheat temperature largely determine the combustion synthesis of Ni-Ti intermetallic material. The samples have to be preheated above a specific temperature to be ignited by the tungsten ignition wire placed on the top surface. This implies that the reactions between Ni and Ti are not sufficiently exothermic for self-sustainable flame propagation.

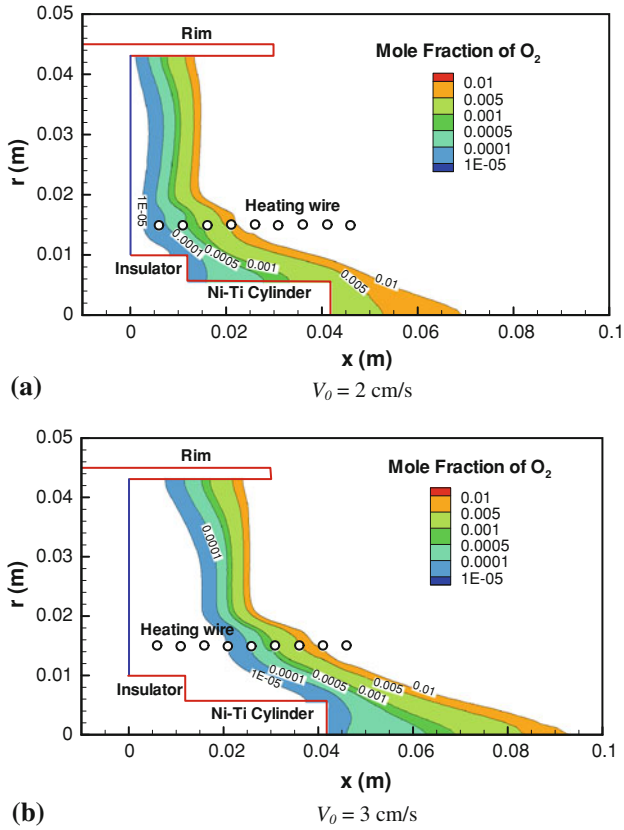

Fig. 4 Contours of mole fraction of oxygen for V_0 = 2 and 3 cm/s in high preheating state

Figure 5 shows a typical SHS process recorded by the motion camera at different instances, using the cylindrical sample of 35% initial porosity that was preheated to 550 °C. After ignition, a bright and self-sustained flame front propagates downward as a nearly parallel (one-dimensional similarity) flame front from the ignited top surface and transforms the preheated reactant into an incandescent combustion product. The flame front propagation velocity was found to be approximately constant, based on the flame front trajectory extracted from the motion camera frames, which was set up to take 50 frames/s at an exposure of 1/200 s. It took approximately 2 s for the flame front to travel from the top of the sample to the bottom over a length of 2.8 cm. The sample was observed to continue to glow and melt down even after 2.8 s. After 5 s, the luminosity on the sample gradually faded away because of the heat loss to the environment. This phenomenon indicates that the flame propagation speed was much larger than the reaction front propagation rate. Thus, the reaction zone was not restricted to the flame front, but continued vigorously in the bulk behind the flame front.

An infrared temperature sensor was applied to record the temperature data and the emissivity for Ni-Ti sample surface was set to 0.55. This value was verified by the thermocouple measurement when the sample surface was heated to 700 °C. However, the emissivity data varied with the surface temperature, especially when the sample started to burn and melt, and so the error in the recorded temperature for the combusted high temperature surface was relatively high (20 °C). Figure 6 shows the temperature versus time graph at one point (diameter 1.8 mm) on the top of the cylinder side face for the SHS

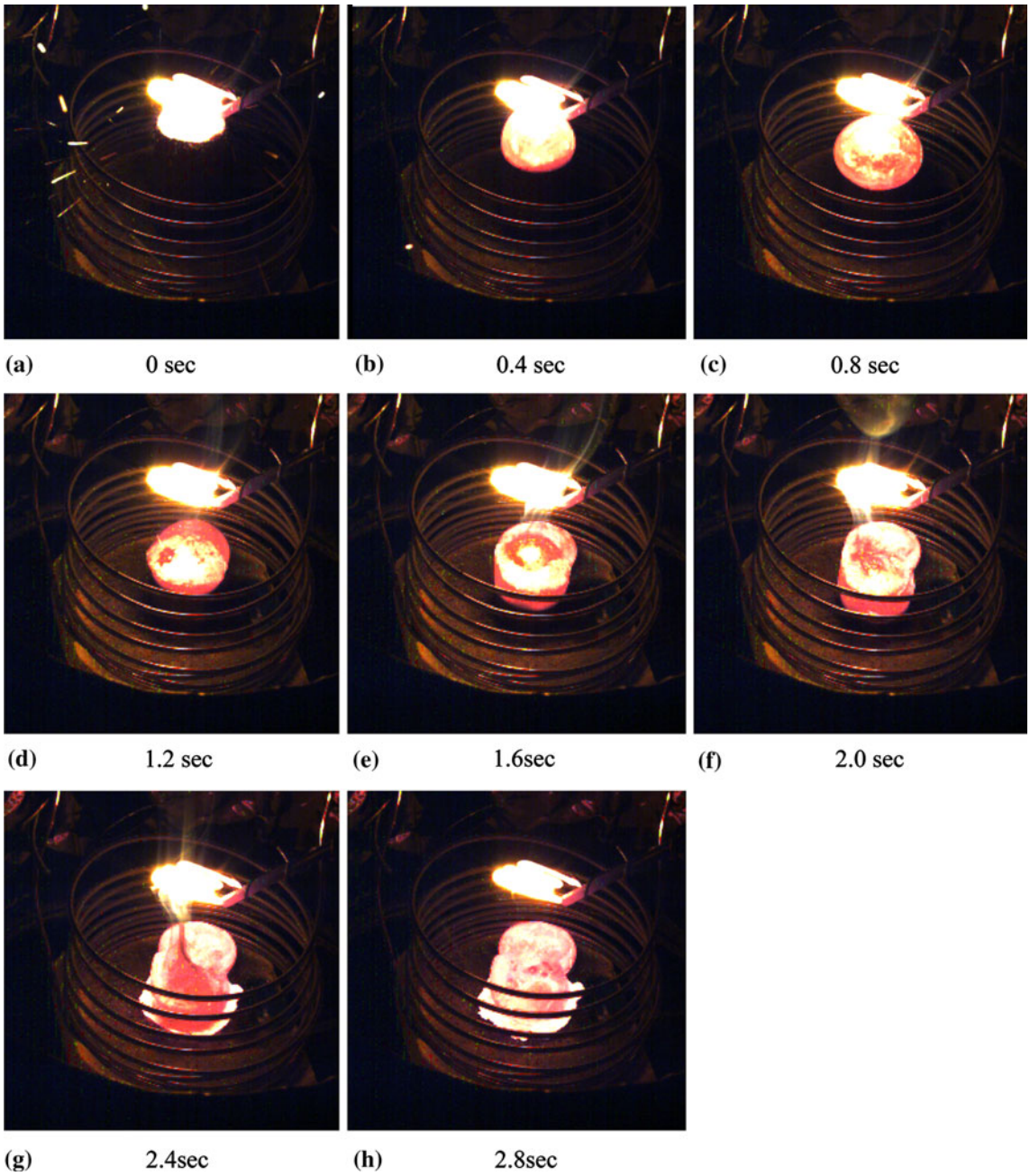

Fig. 5 Recorded combustion synthesis for 35% initial sample porosity, 100 mesh Ni-Ti particles ignited with 550 °C preheating

process utilizing a sample with 35% initial porosity, 100 mesh Ni-Ti particles that was ignited with 550 °C preheating. The sample was slowly preheated to 550 °C, and then the ignition power was abruptly turned on. The sample top surface became heated to 900 °C within 60 s.

Figure 7 is an amplified version of the Fig. 6 with focus on the time duration about 570-571 s. This figure shows the temperature distribution in the system as the flame propagates through that layer. The temperature increases from 920 °C (ignition temperature for Ni-Ti particle mixture; Ref 4, 11) to 1310 °C within 0.1 s, remains flat around 1310 °C for a short period, and increases to 1460 °C after 0.8 s. This is because the Ni-Ti alloy absorbes the latent heat from the exothermic reactions at the melting point (1310 °C). After approximately 0.8 s, the exothermic reactions terminate, and the bulk begins to cool down because of heat loss. Meanwhile, the flame front has propagated over a distance of 2.8 cm × 0.8 s/2.0 s = 1.12 cm, which is the solid flame thickness. However, the temperature increase is concentrated in the flame front layer of thickness 2.8 cm × 0.06 s/2.0 s = 0.84 mm, resulting in a temperature gradient of (1270-920 °C)/0.84 mm = 417 °C/mm. As the flame front propagates downward, the temperature difference on the flame front will be even larger because this zone is not heated by the tungsten ignition wire. The region remains approximately at the preheat temperature of 550 °C before the flame front approaches and initiates the reactions. Therefore, the thermal conductivity and heat transfer in the preheated layer (i.e., the zone from 550 to 920 °C) and flame front layer (920-1270 °C) are critical to the flame front propagation velocity. The thermal conductivity and heat

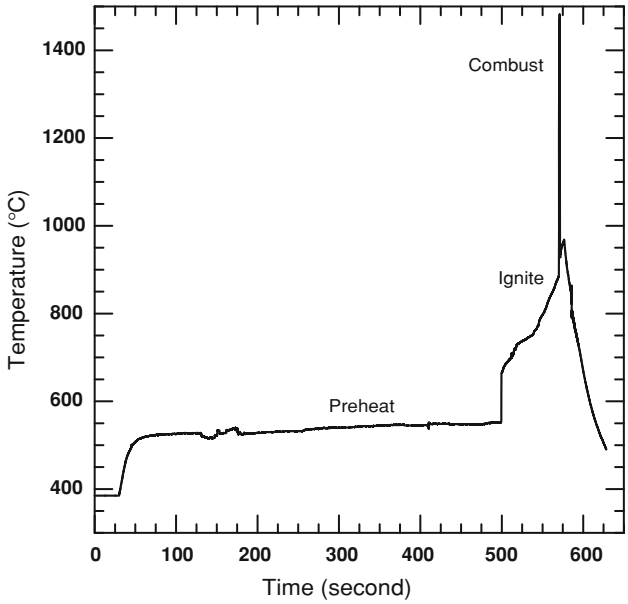

Fig. 6 Temperature vs. time curve of sample surface for SHS with 35% initial sample porosity, 100 mesh Ni-Ti particles ignited with 550 °C preheating

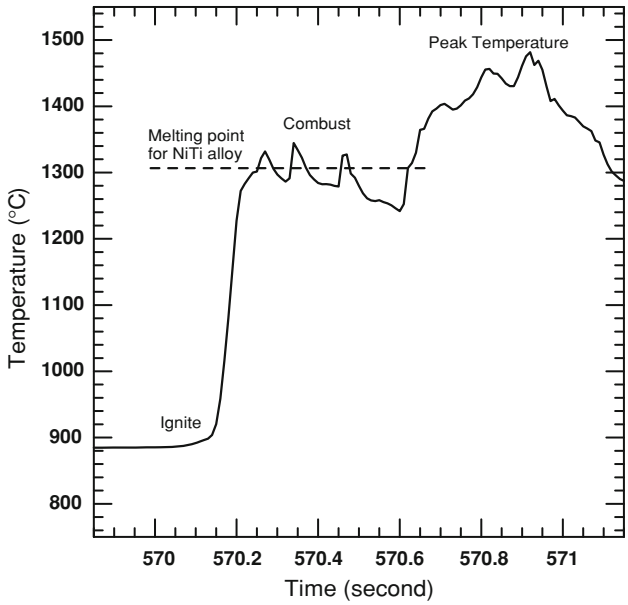

Fig. 7 Amplified temperature vs. time curve of the sample surface for 35% initial sample porosity, 100 mesh Ni-Ti particles ignited with 550 °C preheating

transfer in the flat temperature region comprising the melted Ti-Ni alloy do not appear to be important.

Figure 8 shows the phase diagram of a Ni-Ti binary system, indicating that the lowest eutectic temperature of 942 °C occurs at the Ni-3Ti combination, corresponding to the maximum solubility of Ni in β-Ti. This value also approximately equals to the experimental ignition temperature in this study. Thus, it could be assumed that the beginning of the Ni-3Ti combination and melting effectively triggered the liquid-solid reactions, and most of the raw materials then reacted at the melting point of Ni-Ti of 1310 °C.

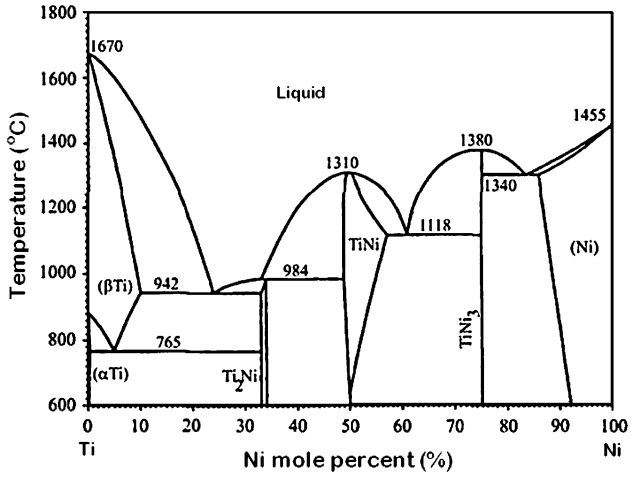

Fig. 8 Phase diagrams of Ni-Ti binary system

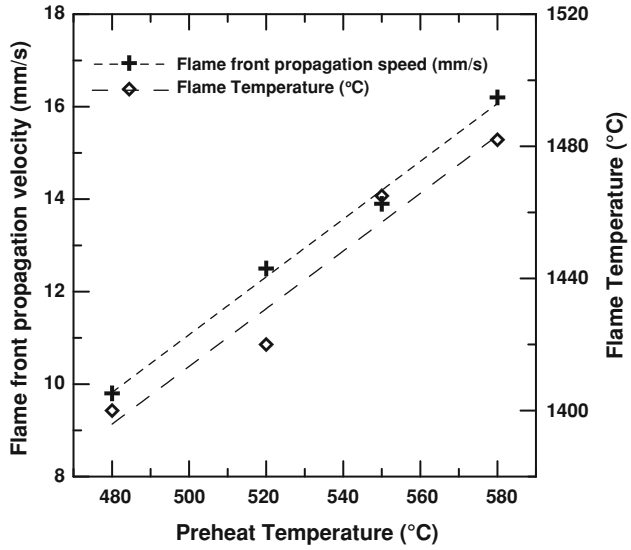

Fig. 9 Dependence of combustion front velocity and product temperature on preheat temperature for the 35% initial porosity, 100 mesh particle size

The higher preheat temperature indicates a smaller temperature barrier between the green reactant and the ignition point. Thus, for the same thermal conductivity the flame front propagation velocity will be significantly increased at the higher preheat temperature. Figure 9 shows the dependence of the flame front velocities and product temperatures on preheat temperature for the sample with 35% initial porosity. The flame front velocities monotonously increase from 9.8 to 16.2 mm/s, when the preheat temperature increases from 480 to 580 °C. The measured product maximum surface temperature which has an error of ±20 °C for the liquid alloy surface (>1310 °C) agrees satisfactorily with the preheat temperature.

For a specified temperature range (e.g., from the preheating temperature 550 °C to the ignition temperature 920 °C) and particle composition (Ni:Ti = 1:1, and 100 mesh size), the average effective thermal conductivity k_{eff} is largely determined by the initial porosity (Ref 4, 22). In particular, the effective

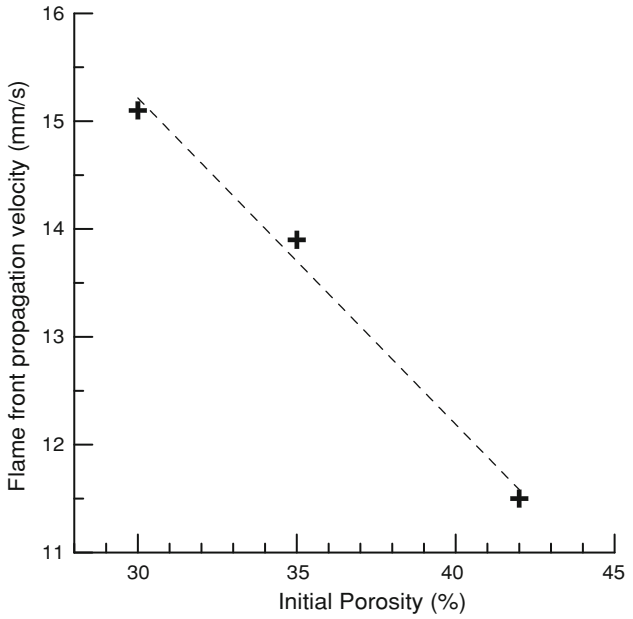

Fig. 10 Dependence of combustion front velocity on initial cylindrical sample porosity with 550 °C preheating

thermal conductivity was observed to linearly decrease approximately with increasing porosity in the range 25-50% (Ref 4, 22). Figure 10 shows the variation of the measured flame front propagation velocity with the initial sample porosity. The flame front velocity increases linearly with decreasing initial sample porosity, which corresponds to increasing k_{eff}. Thus, the flame speed observed in the present experiment could be said to linearly increase with the effective thermal conductivity of the reactant. This observed trend is in the consensus of the experimental data obtained on cobalt-aluminide (CoAl) combustion synthesis (Ref 3).

6. Conclusions

The combustion synthesis of Ni-Ti was investigated experimentally, including the ignition process and flame propagation phenomena. Cylindrical samples were utilized, and the flame propagation was measured as a function of the preheat temperature and initial sample porosity. The major findings of the study can be summarized thus:

- The Ni-Ti system is best ignited by a triggering temperature of 920 °C, which is approximately 20 °C below the lowest eutectic temperature of Ni-3Ti. The eutectic melting accelerates the liquid-solid chain reaction, leading to the bulk Ni-Ti synthesis.
- High preheating temperature and low initial porosity both increase the flame front propagation speed. Low initial porosity increases the effective thermal conductivity of the reactant, and thus, enhances the heat transfer from the reaction zone to the preheating zone. This heat flux heats up the preheating zone to the ignition point (920 °C) and, finally, turns it into the reaction zone, while the flame front propagates ahead.

Acknowledgment

This study was supported by the US National Science Foundation under contract number NSF-CMMI-0854208.

References

1. H.C. Yi and J.J. Moore, The Combustion Synthesis of Ni-Ti Shape Memory Alloys, *J. Miner. Met. Mater. Soc.*, 1990, **42**(8), p 31–35
2. Y. Lu and M. Hirohashi, Thermal Behavior During Combustion Synthesis of Intermetallic Compound of Ni-Al System, *J. Mater. Sci. Lett.*, 1999, **18**(5), p 395–398
3. C.L. Yeh and C.C. Yeh, Preparation of CoAl Intermetallic Compound by Combustion Synthesis in Self-Propagating Mode, *J. Alloys Compd.*, 2005, **288**, p 241–249
4. C. Zanotti, P. Giuliani, A. Terrosu, S. Gennari, and F. Maglia, Porous Ni-Ti Ignition and Combustion Synthesis, *Intermetallics*, 2007, **15**, p 404–412
5. A. Biswas, Porous NiTi by Thermal Explosion Mode of SHS: Processing, Mechanism and Generation of Single Phase Microstructure, *Acta Mater.*, 2005, **53**, p 1415–1425
6. B.-Y. Li, L.-J. Rong, Y.-Y. Li, and V.E. Gjunter, Fabrication of Cellular NiTi Intermetallic Compounds, *J. Mater. Res.*, 2000, **15**(1), p 10–13
7. S.B. Margolis, The Asymptotic Theory of Gasless Combustion, *Metall. Trans.*, 1992, **23A**(1), p 15–22
8. Y. Zhang and G.C. Stangle, A. Micromechanistic Model of the Combustion Synthesis Process. Part I. Theoretical Development, *J. Mater. Res.*, 1994, **9**(10), p 2592–2604
9. J. Puszynski, V.K. Jayaraman, and V. Hlavacek, A Stefan Problem for Exothermic Non-Catalytic Reactions, *Int. J. Heat Mass Transfer*, 1985, **28**(6), p 1237–1239
10. L. Rao, P. Yu, and R.B. Kaner, Numerical Modeling of Combustion Synthesis with Phase Changes, *J. Mater. Synth. Process.*, 1994, **2**(6), p 343–353
11. N. Bertolino, M. Monagheddu, A. Tacca, P. Giuliani, C. Zanotti, and U.A. Tamburini, Ignition Mechanism in Combustion Synthesis of Ti-Al and Ti-Ni Systems, *Intermetallics*, 2003, **11**, p 41
12. H.C. Yi and J.J. Moore, Combustion Synthesis of TiNi Intermetallic Compounds. Part 1. Determination of Heat of Fusion of TiNi and Heat Capacity of Liquid TiNi, *J. Mater. Sci.*, 1989, **24**(10), p 3449–3455
13. H.C. Yi and J.J. Moore, Combustion Synthesis of TiNi Intermetallic Compounds. Part 2. Effect of TiO_2 Formation, *J. Mater. Sci.*, 1989, **24**(10), p 3456–3462
14. A.H. Advani, N.N. Thadhani, H.A. Grebe, R. Heaps, C. Coffin, and T. Kottke, Dynamic Modelling of Material and Process Parameter Effects on Self-Propagating High-Temperature Synthesis of Titanium Carbide Ceramics, *J. Mater. Sci.*, 1992, **27**, p 3309–3317
15. A.K. Bhattacharya, Modelling of the Effects of Porosity and Particle Size on the Steady-State Wave Velocity in Combustion Synthesis, *J. Mater. Sci.*, 1992, **27**(6), p 1521–1527
16. A.K. Bhattacharya, Green Density of a Powder Compact and Its Influence on the Steady-State Wave Velocity in Combustion Synthesis of Condensed Phase, *J. Am. Ceram. Soc.*, 1991, **74**(9), p 2113–2116
17. M.G. Lakshmikantha, A. Bhattacharya, and J.A. Sekhar, Numerical Modeling of Solidification Combustion Synthesis, *Metall. Trans.*, 1992, **23A**(1), p 23–34
18. J. Puszynski, J. Degreve, and V. Hlavacek, Modeling of Exothermic Solid-Solid Noncatalytic Reactions, *Ind. Eng. Chem. Res.*, 1987, **26**(7), p 1424–1434
19. D.M. Matson and Z.A. Munir, Combustion Synthesis of Intermetallic Compounds Using Titanium Nickel and Copper Wires, *Mater. Sci. Eng.*, 1992, **153A**(1/2), p 700–705
20. Y. Zhang and G.C. Stangle, A Micromechanistic Model of the Combustion Synthesis Process. Part II. Numerical Simulation, *J. Mater. Res.*, 1994, **9**(10), p 2605–2619
21. M. Ballas, H. Song, and O.J. Ilegbusi, Effect of Thermal Conductivity on Reaction Front Propagation During Combustion Synthesis of Intermetallics, *J. Mater. Sci.*, 2006, **41**, p 4169–4177
22. X. Huai, W. Wang, and Z. Li, Analysis of the Effective Thermal Conductivity of Fractal Porous Media, *Appl. Therm. Eng.*, 2007, **27**, p 2815–2821